Final Technical Report for USGS National Earthquake Hazards Reduction Program

Award No. G15AP00069

Project Title:	Improved estimation of site response using random vibration theory
Project Term:	May 1, 2015 through April 30, 2016
Principal Investigators:	Gabriel Toro and Andrew Seifried Lettis Consultants International, Inc. 1981 N. Broadway, Suite 330 Walnut Creek, CA 94596 (925) 482-0360, Toro@lettisci.com
Authorized Institutional Representative:	Kevin B. Clahan Lettis Consultants International, Inc. 1981 N. Broadway, Suite 330 Walnut Creek, CA 94596 (925) 482-0360, (925) 482-0361, Clahan@lettisci.com

ABSTRACT

Improved estimation of site response using random vibration theory

Gabriel Toro and Andrew Seifried
Toro@lettisci.com; Seifried@lettisci.com

Site-specific seismic hazard analysis accounts for the effect of local geologic conditions on the expected frequency content of ground motions at a site. This analysis typically involves the propagation of ground motions defined for underlying rock conditions through a soil profile to the surface. This is commonly and efficiently accomplished in engineering practice using a random vibration theory (RVT)-based equivalent-linear approach. Recent research demonstrates that site-specific response spectrum amplification factors (*AF*) obtained using the "duration" RVT approach can be conservative by as much as 50% relative to those obtained using time history methods for some frequencies. A "bandwidth" RVT-based approach to calculating AF is used here to reduce unnecessary conservatism while maintaining computational efficiency. The duration approach uses empirical adjustments to input ground motion duration to compute response amplitude. However, such adjustments do not account for the increase in time history duration observed as real time histories propagate through the soil which leads to overestimation of surface response, particularly at the modal frequencies of the site. The bandwidth approach instead focuses on the response bandwidth of the combined soil- and single-degree-of-freedom (SDOF) system. A theoretical nonstationarity factor replaces empirical duration adjustment to account for the difference between the input ground motion duration and the time required to excite the combined system. These modifications result in estimates of *AF* that are in better agreement with time history methods, particularly at the modal frequencies of the site. Better agreement with time history methods also results in some frequencies where *AF* from the bandwidth approach is increased over the duration approach. The impact of these approaches to probabilistic site response analysis and hazard calculations is also investigated, where it is observed that the net effect of the alternative approaches is mixed. While the bandwidth approach to RVT site response analysis is a theoretically sound alternative to the empirical adjustments of the duration approach, the selection of one or the other in a real-world application will not have a significant impact on the design or retrofit of structures that require the calculation of site-specific hazard. Limitations of the current study are also discussed.

1.0 Introduction

Site-specific seismic hazard analysis accounts for the effect of local soil conditions on the expected frequency content of ground motions at a site. This typically involves the vertical propagation of ground motions defined for underlying rock conditions through a column of soil to a control point elevation (CPE), which will amplify or de-amplify energy at various frequencies depending on the properties of the soil. Such a site response analysis can be performed either in the time domain or in the frequency domain depending on the needs of the analyst. Nonlinear site response analysis, performed in the time domain, is computationally expensive and difficult to implement in engineering practice, particularly within probabilistic seismic hazard analysis (PSHA) where a large number of time histories consistent with a range of ground motion intensities are often needed. Equivalent-linear (EQL) approximations in the frequency domain (e.g. Kramer, 1996) are much easier to implement and are therefore more popular in engineering situations.

The EQL procedure can be performed with a suite of time histories consistent with the underlying rock response spectrum (e.g., Idriss and Sun, 1992). In this type of analysis, time histories with desired properties and spectral shapes are either selected or simulated, transformed to Fourier amplitude spectra (FAS) and phase spectra, and used to perform the site response analysis. Alternatively, the EQL procedure can be performed using random vibration theory (RVT) (e.g., Boore, 2003), which transforms a response spectrum directly to a FAS without the need for time histories. Because of its increased efficiency and numerous validation studies (e.g., Hanks and McGuire, 1981; EPRI, 1993), the RVT approach is commonly used in PSHA.

The goal of a site response analysis is to estimate response spectrum amplification factors, *AF*, which may then be used to obtain an amplified ("soil") response spectrum at the CPE from the underlying rock response spectrum. *AF* is computed as the ratio of response spectral ordinates, S_a, at an individual frequency, f, between the CPE and underlying rock:

$$AF(f) = \frac{S_a(f)_{\mathrm{CPE}}}{S_a(f)_{\mathrm{Rock}}} \qquad 1$$

Despite the advantages of RVT, recent research demonstrates that estimates of *AF* obtained using this approach can be conservative by as much as 50% relative to those obtained using EQL time history methods (e.g. Rathje and Ozbey, 2006; Kottke and Rathje, 2013; Graizer, 2014; Rathje and Kottke, 2014). It is important to emphasize that the comparison being made in these studies is between two types of EQL analysis. Thus, each employs the same central methodology of using transfer functions to alter FAS (e.g. Kramer, 1996). While there is value in comparing each procedure to nonlinear time-domain methods or real data, a direct comparison of *AF* obtained with EQL time history and RVT approaches highlights the effectiveness of the RVT approach once it is determined that EQL is appropriate. Such a comparison also avoids the associated difficulty of modeling true nonlinear behavior.

Complicating the comparison of EQL techniques in the frequency domain are multiple formulations of the RVT approach to site response based on contributions from Cartwright and Longuet-Higgins (1956), Vanmarcke (1976), Der Kiureghian (1980), and many others since. These are divided into two broad categories denoted herein as the "duration" approach and the "bandwidth" approach. Each approach is described in more detail in the following sections.

The objective of this study is to evaluate alternative formulations of the bandwidth approach to estimating *AF* using RVT that do not rely on empirical adjustments, potentially reduce unnecessary conservatism relative to the time history approach, and maintain computational efficiency. This evaluation is performed for several hypothetical sites and earthquake scenarios. The impact of duration and bandwidth RVT approaches to site response analysis on PSHA results is also investigated.

2.0 Background of RVT approaches to site response

The calculation of a transfer function between the input and output elevations of a soil column is common to all site EQL site response analysis approaches. In the time history approach, a number of individual time histories are multiplied by this transfer function in the frequency domain, converted back to the time domain, and used to calculate amplified response spectra. This is typically performed for a suite of time histories such that the mean amplified response spectrum and/or mean *AF* can be computed. The main advantage of RVT-based approaches over the time history approach is that time histories are not required. RVT provides a direct estimate of the mean amplified response spectrum in a single calculation.

Boore (2003) describes a commonly applied approach to derive a response spectrum from a FAS using RVT. It is briefly presented here, and further details may be found in that work, Rathje and Ozbey (2006), or many others. Areas relevant to the proposed alternative approach receive the most focus.

The approach to estimating the maximum of a random response variable *Y* using RVT is assumes that the response is a finite-duration segment of a stationary Gaussian process, obtaining

$$y_{max} = pf \times y_{rms} \qquad 2$$

where y_{max} is the maximum response (in this case y_{max} is equivalent to S_a), y_{rms} is the root-mean-square (rms) valus of the stationary response, and *pf* is a peak factor. y_{rms} is derived from Parseval's theorem

$$y_{rms} = \sqrt{m_0/D_{rms}} \qquad 3$$

where m_0 is the 0th moment of the Fourier energy spectrum of the response and D_{rms} is the response duration. Moments of the response Fourier energy spectrum are defined by

$$m_k = 2\int_0^\infty (2\pi f)^k |A(f)|^2 |H(f)|^2 df \qquad 4$$

where *A(f)* denotes the Fourier amplitude of the ground motion at frequency *f*, and *H* is the frequency response function of an SDOF oscillator.

The peak factor of Boore (2003) is based on Cartwright and Longuet-Higgins (1956) and is defined by

$$pf = 2\int_0^\infty \left(1 - \left[1 - \frac{N_z}{N_e}\exp(-z^2)\right]^{N_e}\right) dz \qquad 5$$

where N_z is the expected number of zero crossings and N_e is the expected number of extrema. They are defined by

$$N_z = 2f_z T_{gm} \qquad N_e = 2f_e T_{gm}$$
$$f_z = \frac{1}{2\pi}\sqrt{\frac{m_2}{m_0}} \qquad f_e = \frac{1}{2\pi}\sqrt{\frac{m_4}{m_2}} \qquad 6$$
$$\xi = \frac{N_z}{N_e} = \sqrt{\frac{{m_2}^2}{m_0 m_4}}$$

The integration of the peak factor (Eq. 5) has the asymptotic form for large N_z of

$$pf \approx \sqrt{2\ln(N_z)} + \frac{0.5772}{\sqrt{2\ln(N_z)}} \qquad 7$$

In general the peak factor integration is well-behaved numerically and easy to implement, but there is little difference between the peak factors predicted in each manner (e.g., Rathje and Ozbey, 2006).

2.1 Duration approach

It is important to distinguish between the strong-motion duration of the ground motion, D_{gm}, and the duration of the response, D_{rms} in Eqn. 3. Note that D_{rms} will always be at least as long as D_{gm} because the SDOF system will often continue to vibrate after the ground motion has stopped (e.g. Boore and Joyner, 1984), but it will not end before the ground motion ends. The assumption of stationarity mentioned above, implicit in Equations 2-7, is valid only when the SDOF oscillator period is of the same order as, or shorter than, D_{gm}.

In the duration approach, the quantity D_{rms} has received much attention by those attempting to improve its agreement with EQL time history methods when the assumption of stationarity is not satisfied (e.g. Boore and Joyner, 1984; Liu and Pezeshk, 1999; Boore and Thompson, 2012). Note that m_0 is a measure of the system response energy, which in Eq. 2 is spread over D_{rms}. A large value of D_{rms} will yield a smaller value of y_{rms} and therefore also y_{max}. The opposite is also true, where a shorter D_{rms} will yield a larger y_{max}. Proper specification of this duration is critical to obtaining appropriate response spectral ordinates.

Boore and Joyner (1984) developed an empirical model to obtain D_{rms} when the SDOF oscillator period of the same order as, or longer than, D_{gm}.

$$\gamma = D_{gm} f$$
$$D_{rms} = D_{gm} + \left(\frac{\gamma^3}{\gamma^3 + {}^1/_3}\right)\frac{1}{2\pi f \beta} \qquad 8$$

in which β is the oscillator damping ratio.

The correction factors of Boore and Joyner (1984), Liu and Pezeshk (1999), and Boore and Thompson (2012) do well to capture the increase in response duration of SDOF oscillators to ground motion excitation, but they do not account for the increase in duration of the time history as it propagates through the soil column. This can lead to significant underestimation of the response duration, especially at resonant frequencies of the soil column, leading to overestimation of amplified spectra (e.g. Kottke and Rathje, 2013; Rathje and Kottke, 2014; Seifried and Toro, 2015; Wang and Rathje, 2016).

2.2 Bandwidth approach

A drawback of the duration approach is that it requires an empirical adjustment for the increased oscillator response duration relative to the ground motion duration. As noted above, D_{rms} tends to increase as waves propagate through the soil, particularly at the modal frequencies of the site, so it must also be considered in the correction. So far, these empirical adjustments do not also account for the additional increase in duration due to the soil column.

The alternative bandwidth approach is a theoretical departure to the empirical adjustment of duration that considers the coupled soil-SDOF system and accounts for their combined response to achieve better agreement with EQ time history methods. There are two components of this alternative approach: how to address the effect of nonstationarity on the calculation of y_{rms}, and the calculation of *pf*.

Because a correction for D_{rms} is not required for this approach, D_{rms} is replaced with D_{gm} in the definition of y_{rms} above (Eq. 2). A nonstationarity factor, *nf*, is instead included to account for the ratio between the rms value of the nonstationary response at the end of the excitation to the stationary rms response level (Vanmarcke, 1976; Toro, 1984)

$$y_{rms} = pf \times nf \times \sqrt{m_0/D_{gm}} \qquad 9$$

where

$$nf = \sqrt{1 - \exp\left(-4\pi\beta f D_{gm}\right)} \qquad 10$$

The nonstationarity factor is typically less than 1.0 for low-frequency spectral ordinates coupled with short strong-motion durations, which is analogous to the increase in duration for the duration approach above.

Vanmarcke (1976) demonstrates that an effective damping parameter β' (Eq. 10) can be related to the bandwidth δ (Eq. 11), which is obtained through moments of the response Fourier energy spectrum using

$$\beta' = \frac{\pi\delta^2}{4} \qquad 11$$

$$\delta = \sqrt{1 - \frac{m_1^2}{m_0 m_2}} \qquad 12$$

Note that in this report, the moments of the response Fourier energy spectrum include the energy of the input ground motion, the transfer function of the soil column, and the frequency-response function of oscillator. Therefore, δ represents the bandwidth of the combined soil-SDOF oscillator system, and β' represents the effective damping associated with that bandwidth.

Der Kiureghian (1980) and EPRI (1988) provide an additional modification to replace N_z in the asymptotic equation for *pf* (Eq. 7) with an equivalent number of cycles *N* such that

$$N = \max(N_z(1.63\delta^2 - 0.38), 1.33) \qquad 13$$

The minimum value of 1.33 introduced in EPRI (1988) for *N* ensures that the peak factor will not fall below $\sqrt{2}$, the peak factor of a sinusoid. Vanmarcke (1976) discusses the correlation of peak responses in time as response bandwidth narrows. Modification of the number of cycles via a bandwidth parameter takes into account this correlation and reduces *N* to a more appropriate level. This has the effect of reducing the peak factor, and therefore also y_{max} by Eq. 2.

2.2.1 Different measures of bandwidth

The bandwidth parameter δ identified in Eqn. 12 is derived from what is essentially a weighted average of the power spectral density function of the soil-SDOF response. It is a single value used to succinctly parameterize complex response frequency content. The tradeoff with its simplicity is that it results in a loss of information. Other parameters obtained using slightly different derivations also exist, and are well-summarized in Winterstein and Cornell (1985). Two alternative bandwidth parameters presented in their work are included in this analysis. The first uses higher moments of the soil-SDOF response FAS

$$\epsilon = \sqrt{1 - \frac{m_2^2}{m_0 m_4}} \qquad 14$$

The second is based on the energy fluctuation scale of the response, θ_E, which is calculated by

$$\theta_E = \frac{4}{m_0^2}\int_0^\infty |A(f)|^4 |H(f)|^4 \, df \qquad 15$$

The associated measure of effective system damping using this parameter is

$$\beta' = \frac{1}{2\pi f_z \theta_E} \qquad 16$$

which implies a bandwidth parameter of

$$\varphi = \frac{1}{\pi}\sqrt{\frac{2}{f_z \theta_E}} \qquad 17$$

δ, ϵ, and φ differ in their sensitivity to high-frequency response components, which influences their effectiveness in capturing characteristics relevant to the response spectrum. For example,

because of the inclusion of the moment, ϵ does not exist for the response of an SDOF oscillator to white noise input. φ is the least sensitive to high-frequency components.

These bandwidth parameters are each used here to adjust damping in the calculation of *nf* as well as to modify the equivalent number of cycles *N* of the combined system response. Figure 1a shows an example of a squared FAS of the ground motion after amplification by the soil column with fundamental frequency of 2.5 Hz, a squared 2 Hz SDOF oscillator frequency-response function, and their product, from which the moments of Eqn. 4 are calculated. Bandwidth parameters δ, ϵ, and φ calculated for a range of SDOF oscillator frequencies (and the same soil column) are shown in Figure 1b, the effective number of cycles are shown in Figure 1c, and the associated *pf*, β', and *nf* are shown in Figures 1d, e, and f.

All parameters in Figure 1 reflect the frequency content of the soil-SDOF system response. Bandwidth parameters vary between 0 and 1, where 0 indicates a narrow band response and 1 indicates a broadband response. A smaller bandwidth results in a reduction of the number of cycles *N* due to the correlation of peak responses. This similarly reduces *pf* and therefore also spectral ordinates. Larger bandwidth values do not decrease *N* or *pf*, but this is offset by an increase in effective damping, which will decrease spectral ordinates. When both the number of cycles and bandwidth are low, *nf* is also reduced. This is indicative of a system that doesn't have time to build up to its stationary response level.

Note that δ and ϵ have similar functional forms, but they use different order moments. The higher order moments of ϵ are more sensitive to frequency content further from the SDOF natural frequency, which makes ϵ more likely to have a value close to 1. Conversely, the higher exponent on the product of FAS and *H* in the derivation of φ makes it much less sensitive to frequency content further from the SDOF frequency, even if the FAS doesn't decay quickly.

The effect of each bandwidth parameter on the calculation of *AF* is examined below. The five combinations of parameters that will be compared are highlighted in Table 1.

Table 1. Combinations of parameters used for analysis

Case	**Number of cycles**	***pf***	***nf***
1	*N*z (Eqn. 6)	Eqn. 7	Eqn. 10
2	*N* (Eqn. 13)	Eqn. 7 using *N* in place of N_Z	Eqn. 10
3	*N* (Eqn. 13)	Eqn. 7 using *N*	Eqn. 10 using damping based on δ
4	*N* (Eqn. 13) using ϵ in place of δ	Eqn. 7 using *N*	Eqn. 10 using damping based on ϵ
5	*N* (Eqn. 13) using φ	Eqn. 7 using *N*	Eqn. 10 using damping based on φ
6	*N* (Eqn. 13) using ϵ	Eqn. 7 using *N*	Eqn. 10 using damping based on φ

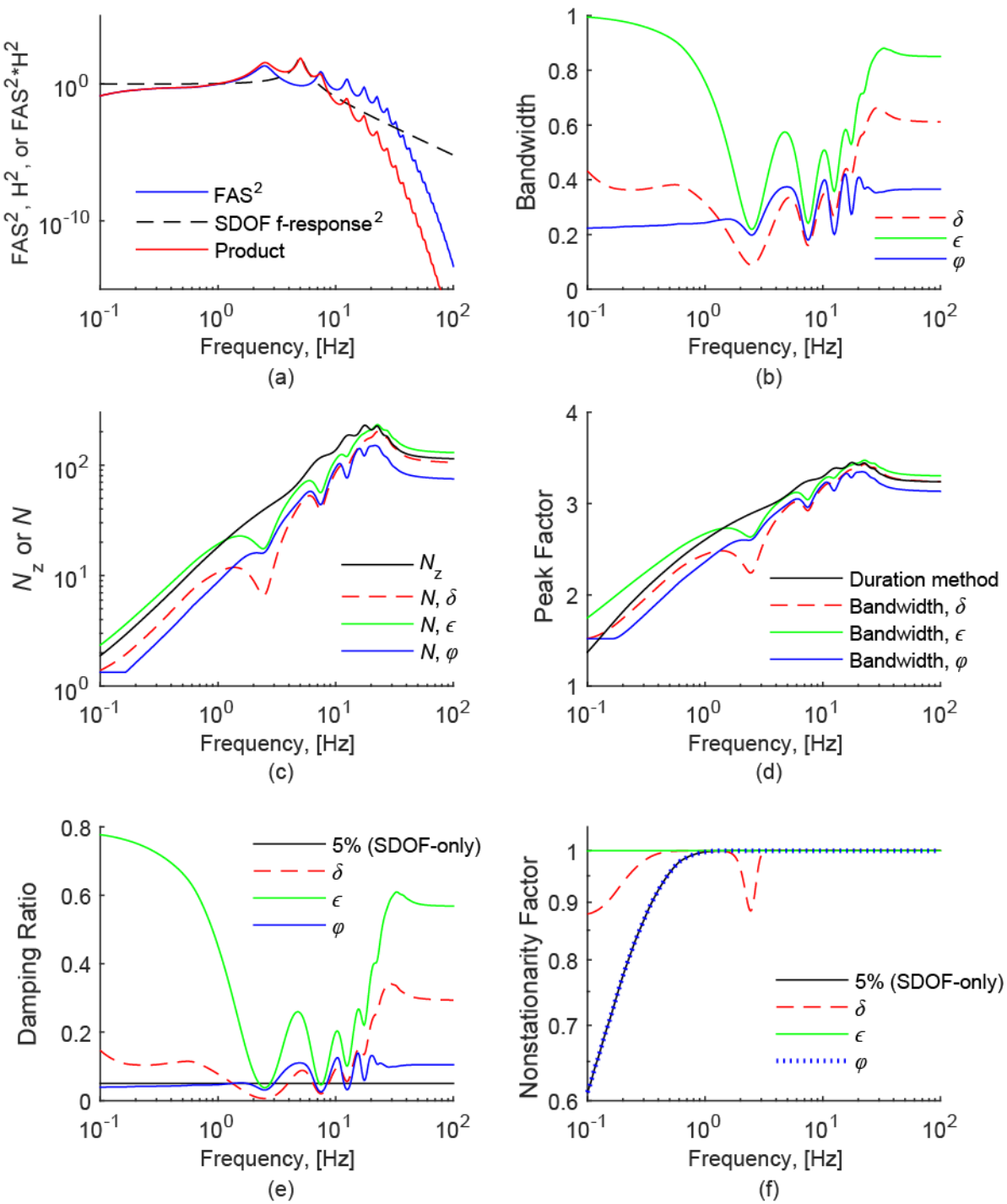

Figure 1. a) An example of a squared FAS of the ground motion after amplification by the soil column with fundamental frequency of 2.5 Hz, a squared 2 Hz SDOF oscillator frequency-response function, and their product; b) bandwidth parameters δ, ϵ, and φ calculated for a range of SDOF oscillator frequencies and the same soil column; c) number of cycles or effective number of cycles; d) *pf*; e) β and β'; f) *nf*.

3.0 Example applications

Four hypothetical one-dimensional elastic soil profiles represented by their shear wave velocity (V_S) in Figure 2 are analyzed using the time history method and the duration and bandwidth RVT methods for three different earthquake scenarios (Figure 3). The scenarios consist of magnitude (M) 5, 6, and 7, each at a distance (R) of 30 km, resulting in different proportions of high and low frequencies. To facilitate time history site-response analyses, 40 time histories are generated for each scenario using SMSIM (Version 6.0, obtained from www.daveboore.com). This deterministic analysis investigates the bias in *AF* resulting from the different approaches and formulations considered. In the following section, a probabilistic analysis incorporates variability in the shear wave velocity profiles in a manner typical of many PSHAs performed in engineering practice (e.g., EPRI, 2013a).

EQL behavior of the profiles is modeled using typical shear modulus and damping values for firm soil. Low-strain damping of the soil is equivalent to 1%, and damping in the linear rock half-space (where V_S = 9200 ft/sec) is set to 0.5%. The variety of profiles in Figure 2 provide a variety of amplification characteristics that are described below.

AF is calculated for the RVT approaches by first computing mean smoothed Fourier amplitude spectra from the suites of time histories at both the top and bottom of the soil. RVT is then used to obtain the associated response spectra, setting D_{gm} to the average 5-75% cumulative energy duration of the suite. Note that D_{gm} calculated from the time histories, and subsequently used in the RVT calculations, will decrease with M.

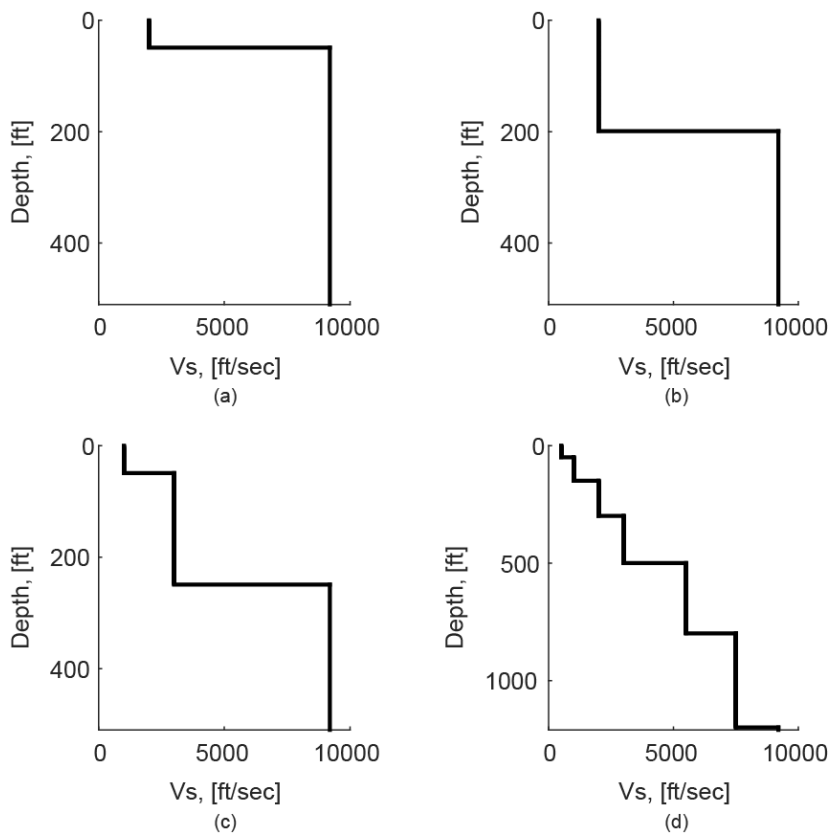

Figure 2. V_S profiles for four hypothetical sites.

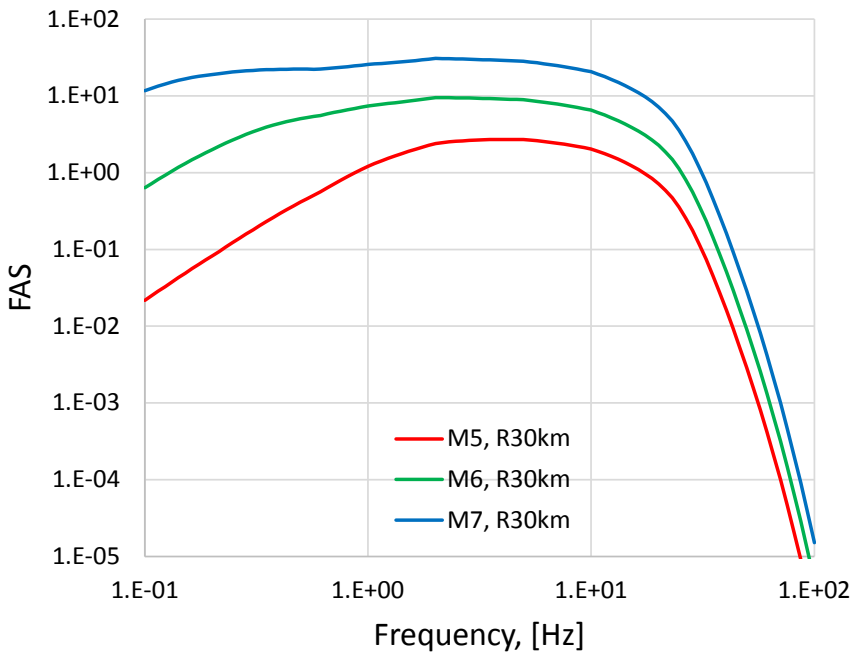

Figure 3. FAS for each of the three analyzed earthquake scenarios.

The duration approach is performed using the integration of *pf* per Eqn. 5 and the duration adjustment of Eqn. 8. Note that more recent duration adjustments from Eqn. 8 (e.g., Liu and Pezeshk, 1999; Boore and Thompson, 2012) are not evaluated here, but this is not expected to have a significant impact on the results of this investigation. The bandwidth approach is performed using a number of different formulations in Table 1 to find an optimal combination of *pf* and *nf*.

Each profile is first analyzed using the M7 R30km scenario. *AF* are computed per Eqn. 1 using mean input and amplified response spectra resulting from the time history approach, duration approach, and bandwidth approach with each parameter case. The resulting *AF* are shown in Figure 4, and ratios of the *AF* obtained using duration and bandwidth approaches to the time history approach are shown in Figure 5, each resulting from the parameters of Case 1 in Table 1 for the bandwidth approach. Note the characteristics of the amplification of each profile in Figure 4: *AF* from Site A is narrowbanded and representative of the strong resonance resulting from a single, sharp impedance contrast; *AF* from Site B includes several higher modes of amplification, achieved by deepening the impedance contrast to lower the resonant frequency of the soil; and *AF* from Sites C and D are more broadbanded due to additional depth and layers.

In the analysis using Case 1 parameters, the bandwidth and duration approaches are consistent. This is because the asymptotic *pf* of Eqn. 7 behaves similarly to the integral of Egn. 5 (e.g., Rathje and Ozbey, 2006). A slight difference exists between *AF* at low frequencies due to the nonstationarity factor of the bandwidth approach and D_{rms} corrections of the duration approach, but it is negligible for this comparison. Note that none of the Case 1 parameters for the bandwidth approach include a bandwidth parameter, which is why *AF* from each approach at the

frequencies amplified by each hypothetical site are equally biased. Neither approach accounts for the nonstationarity of the soil-SDOF system at frequencies amplified by the soil column.

Case 2 of the bandwidth approach us parameters as outlined in EPRI (1988). It is different from Case 1 by the inclusion of the δ bandwidth parameter to adjust the number of cycles and compute *pf*. Results are shown in Figures 6 and 7. The bandwidth adjustments result in much better agreement between *AF* computed at the frequency of peak *AF* for each profile, but there is a slight unconservative bias at those peak frequencies. There is also a systematic overestimation of low-frequency amplification.

Case 3 of the bandwidth approach is different from Case 2 in that it uses the measure of effective damping from the δ bandwidth parameter in the computation of *pf*. Results are shown in Figures 8 and 9. This option exacerbates both the underestimation of *AF* at peak resonances and overestimation of *AF* at low frequencies. This is due to the characteristics of *nf* for δ as illustrated in Figure 1f.

Case 4 of the bandwidth approach is similar to Case 3, but replaces all instances of δ with ϵ. Results are shown in Figures 10 and 11. This formulation of the bandwidth approach represents a real improvement over the duration approach at frequencies amplified by the soil column, and reduces or removes the overprediction of *AF* at low frequencies. The exception to low-frequency overprediction is Site A, which has a strong, narrowband resonance at 10 Hz. When the amplification is more broadbanded or occurs at lower frequencies, the overprediction disappears. Wang and Rathje (2016) point out that the combination of input FAS shape and amplification of the soil can have unintended influence on the bandwidth parameter when the *AF* amplify frequencies that are decaying rapidly. This decay begins at about 10 Hz for the M7 scenario in Figure 3.

Case 5 of the bandwidth approach is similar to Case 4, but it uses adjustments derived from φ. Results are shown in Figures 12 and 13. Low frequency *AF* are in excellent agreement with the time history approach, but the extremes at resonant frequencies are not reduced, and high-frequency *AF* are biased low.

Case 6 of the bandwidth approach combines the peak factor adjustments of ϵ that work very well for *AF* at amplified frequencies and high frequencies, but the nonstationarity adjustment of φ that works well for lower frequencies. Results are shown in Figures 14 and 15. These results are very similar to Case 4, but the incorporation of the bandwidth parameter based on φ improves the low frequency bias for Site D.

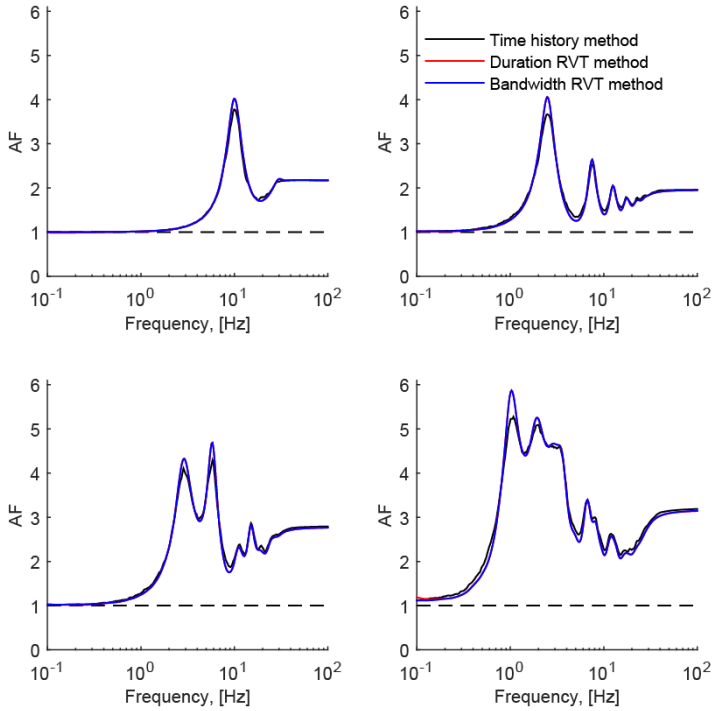

Figure 4. *AF* obtained from each approach for the M7 R30 km scenario. Bandwidth approach uses Case 1 parameters from Table 1. Figures correspond to profiles in Figure 2.

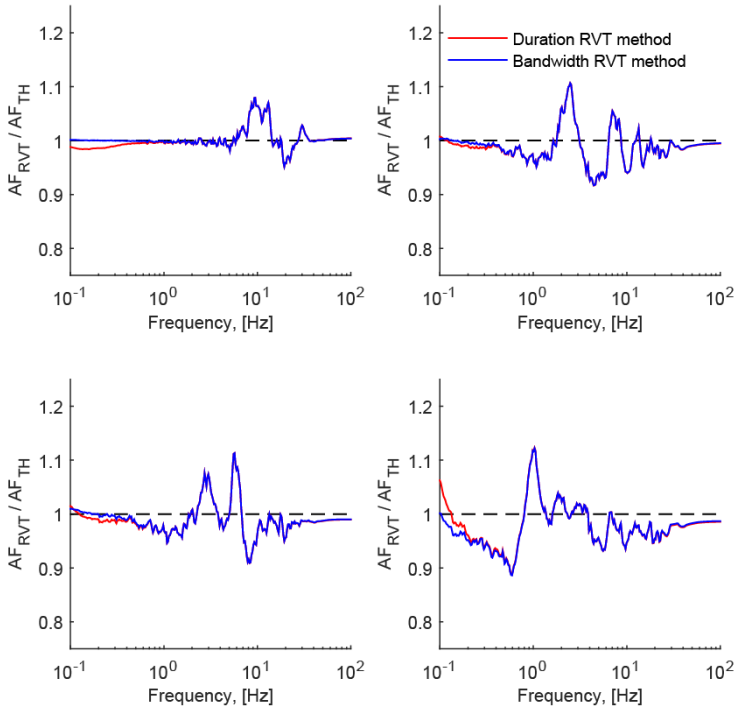

Figure 5. Ratios of *AF* obtained from each RVT approach relative to the time history approach for the M7 R30 km scenario. Bandwidth approach uses Case 1 parameters from Table 1.

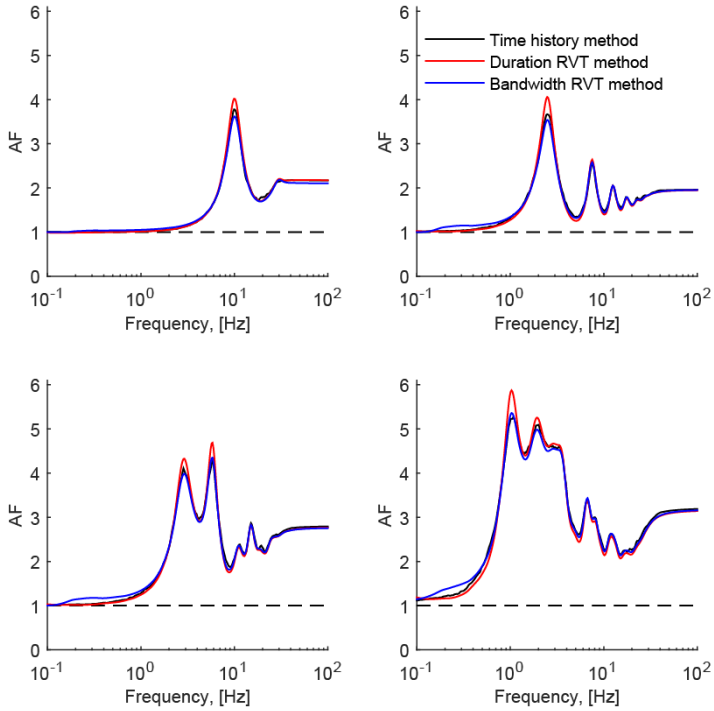

Figure 6. *AF* obtained from each approach for the M7 R30 km scenario. Bandwidth approach uses Case 2 parameters from Table 1. Figures correspond to profiles in Figure 2.

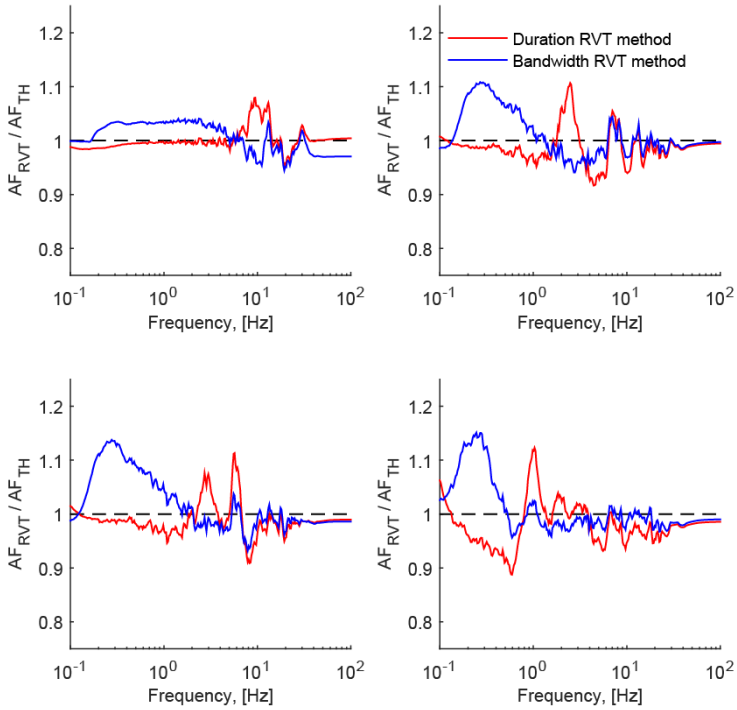

Figure 7. Ratios of *AF* obtained from each RVT approach relative to the time history approach for the M7 R30 km scenario. Bandwidth approach uses Case 2 parameters from Table 1.

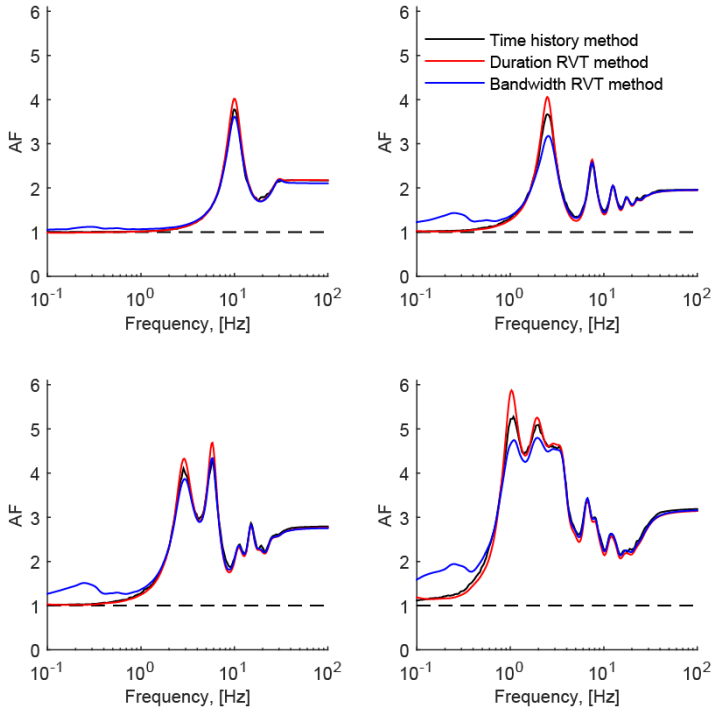

Figure 8. *AF* obtained from each approach for the M7 R30 km scenario. Bandwidth approach uses Case 3 parameters from Table 1. Figures correspond to profiles in Figure 2.

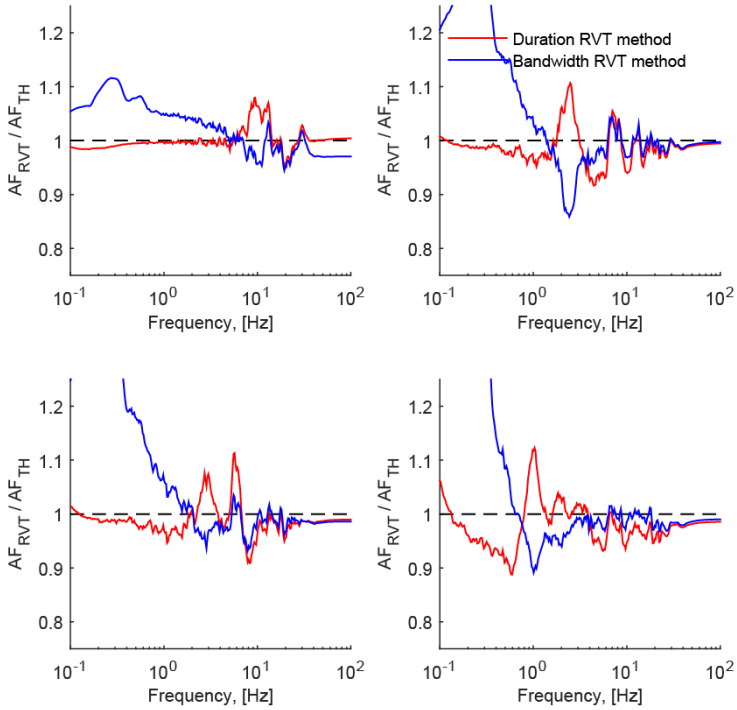

Figure 9. Ratios of *AF* obtained from each RVT approach relative to the time history approach for the M7 R30 km scenario. Bandwidth approach uses Case 3 parameters from Table 1.

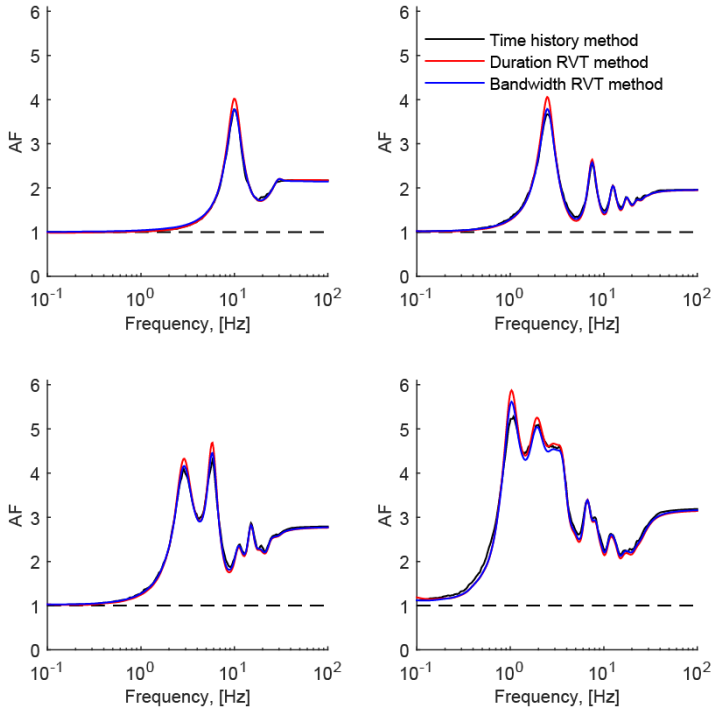

Figure 10. *AF* obtained from each approach for the M7 R30 km scenario. Bandwidth approach uses Case 4 parameters from Table 1. Figures correspond to profiles in Figure 2.

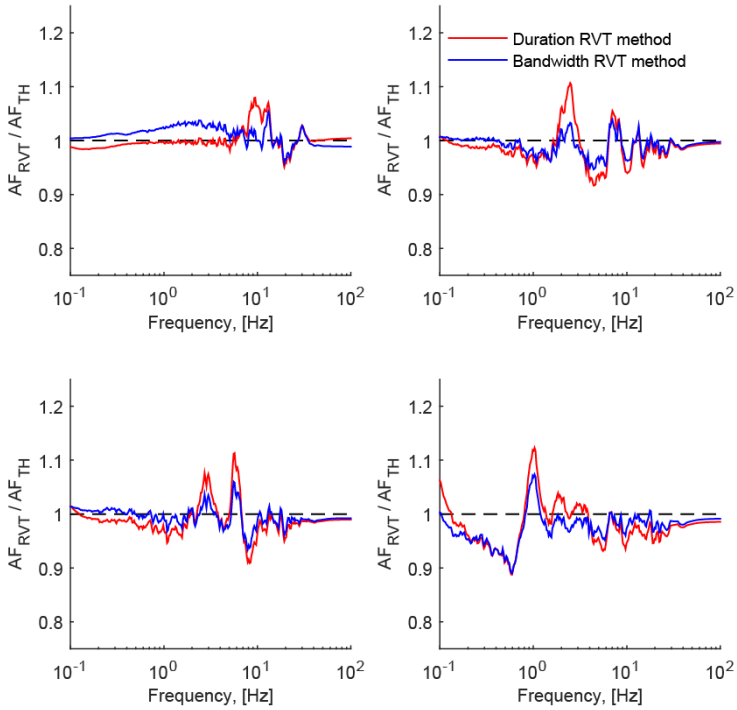

Figure 11. Ratios of *AF* obtained from each RVT approach relative to the time history approach for the M7 R30 km scenario. Bandwidth approach uses Case 4 parameters from Table 1.

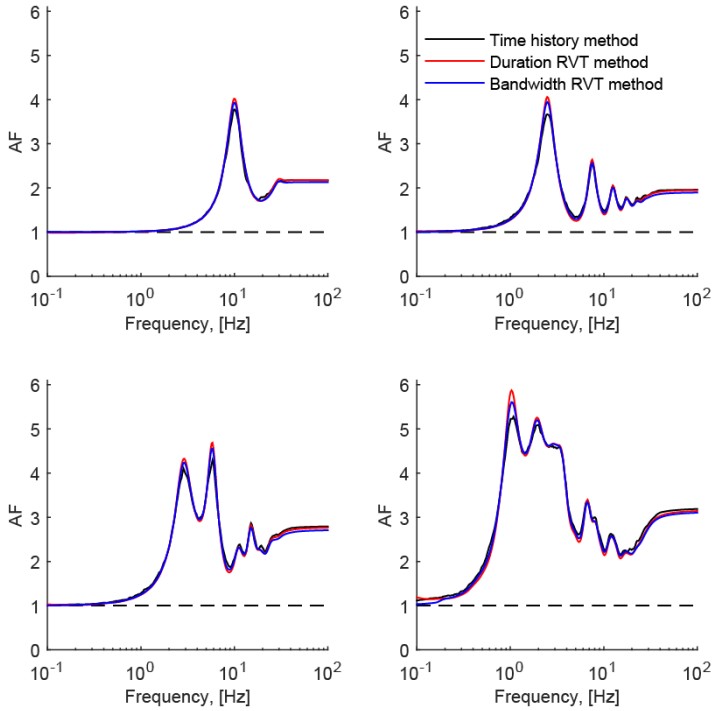

Figure 12. *AF* obtained from each approach for the M7 R30 km scenario. Bandwidth approach uses Case 5 parameters from Table 1. Figures correspond to profiles in Figure 2.

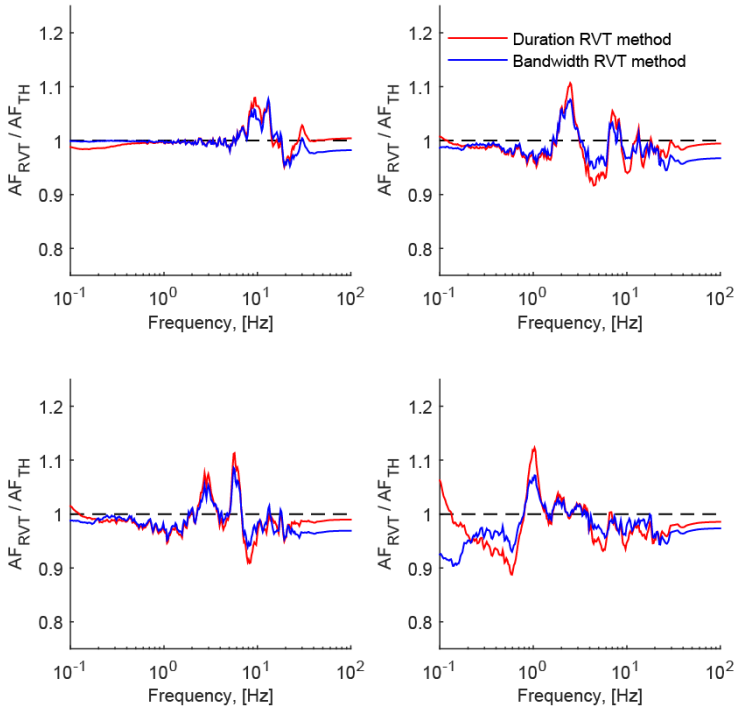

Figure 13. Ratios of *AF* obtained from each RVT approach relative to the time history approach for the M7 R30 km scenario. Bandwidth approach uses Case 5 parameters from Table 1.

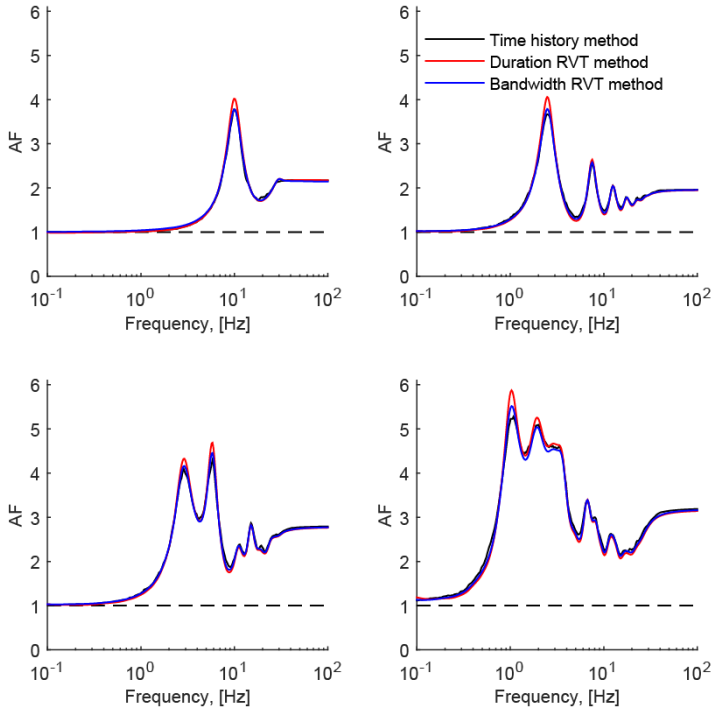

Figure 14. *AF* obtained from each approach for the M7 R30 km scenario. Bandwidth approach uses Case 6 parameters from Table 1. Figures correspond to profiles in Figure 2.

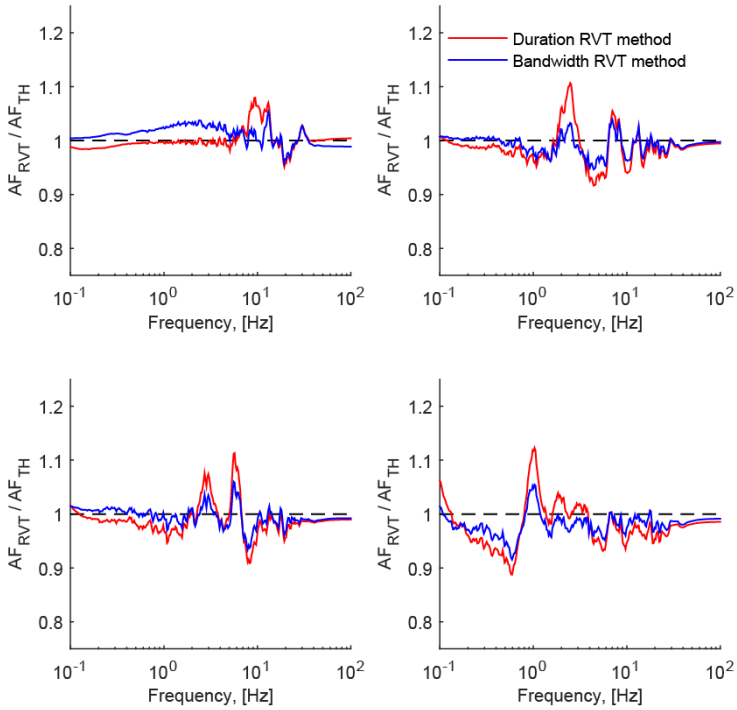

Figure 15. Ratios of *AF* obtained from each RVT approach relative to the time history approach for the M7 R30 km scenario. Bandwidth approach uses Case 6 parameters from Table 1.

The best agreement between the bandwidth approach and time history approach is obtained using Case 6 parameters. The remaining two scenarios (M6 and M5) are analyzed for this parameter case and results are shown in Figures 16 through 19. The same trends observed for the M7 scenario are generally observed here. Discrepancies for low-frequency *AF* are largely due to the short ground motion durations relative to the soil-SDOF system response frequencies. The systems reach only a fraction of their stationary response level.

Considering all scenarios, the time history approach, duration approach, and the bandwidth approach using Case 6 parameters, *AF* generally agree well in terms of predicting amplification of the soil profile. Overprediction of *AF* relative to the time history approach exists for each RVT approach at the peak amplified frequencies of each analyzed site. The degree of overprediction reaches a maximum of about 15% for the duration approach. The ability of the bandwidth approach to parameterize complex and correlated behavior as represented by the energy content of the response of the soil-SDOF system reduces this overprediction of *AF* by factors of two or more at peak amplified frequencies.

As M (and therefore also D_{gm}) decrease, general agreement between time history and RVT approaches deteriorates slightly, particularly at lower frequencies for both RVT approaches. There are two main reasons for this. First, for the M5 and M6 scenarios there is strong low-frequency amplification but little low frequency energy in the time histories (Figure 3). Moments of the energy spectrum for the soil-SDOF system response (Eqn. 4) are sensitive to changes in FAS when they occur just below the corner frequency, and slight changes in the frequency content of this region can impact the predicted spectral ordinate (e.g., Wang and Rathje, 2016). The other reason is that RVT is meant to predict the mean peak of stationary responses to stationary excitation, and both the theoretical and empirical adjustments made in each RVT approach serve to estimate the relatively reduced peak response level of what are nonstationary responses to nonstationary excitations. As D_{gm} decreases, it becomes more difficult to accurately model this reduction. These reasons explain the poor agreement of *AF* in the low-frequency range, however, the deterioration of agreement in *AF* at amplified frequencies for the duration approach is due to the inability of this approach to capture the effect of site amplification characteristics on amplified surface spectra, as described above. This limitation of the RVT approaches is less serious than it appears at first, because the low-frequency response is less important for lower-magnitude earthquakes.

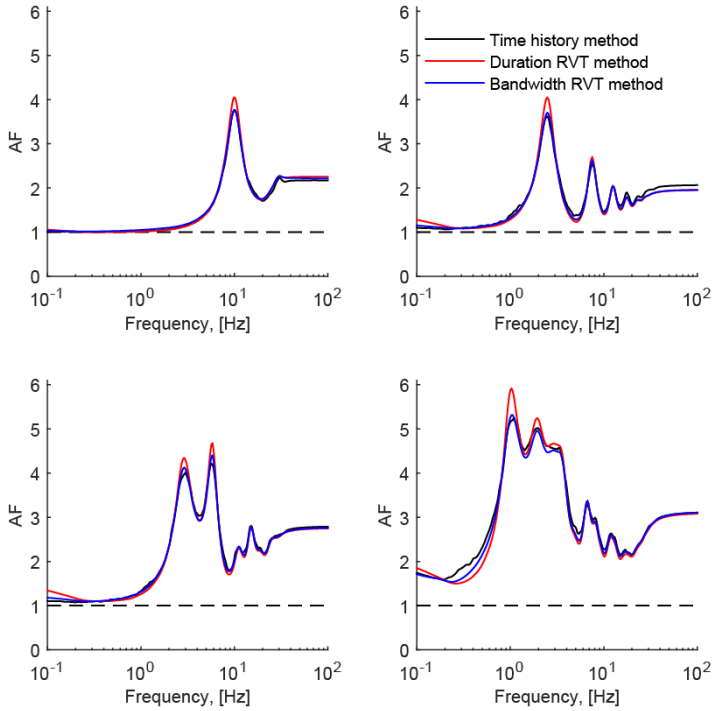

Figure 16. *AF* obtained from each approach for the M6 R30 km scenario. Bandwidth approach uses Case 6 parameters from Table 1. Figures correspond to profiles in Figure 2.

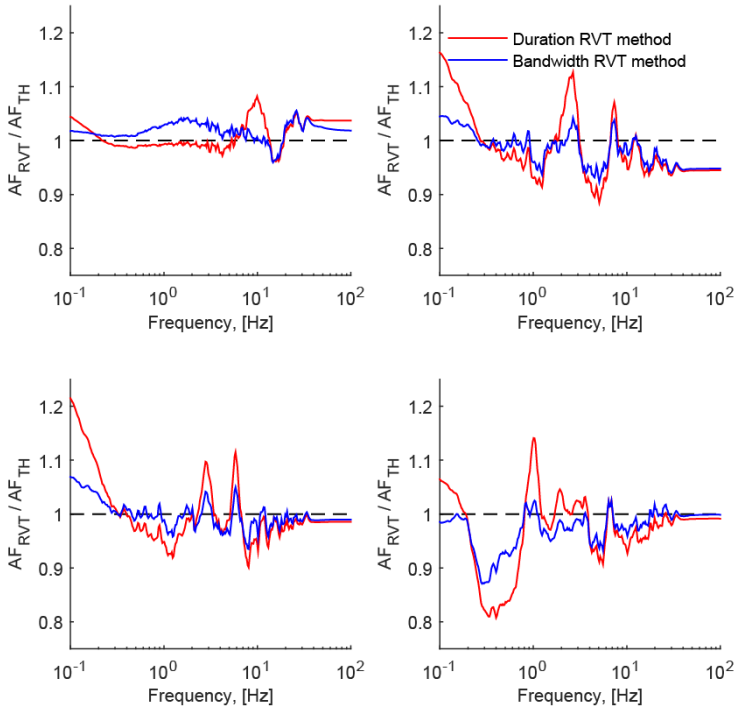

Figure 17. Ratios of *AF* obtained from each RVT approach relative to the time history approach for the M6 R30 km scenario. Bandwidth approach uses Case 6 parameters from Table 1.

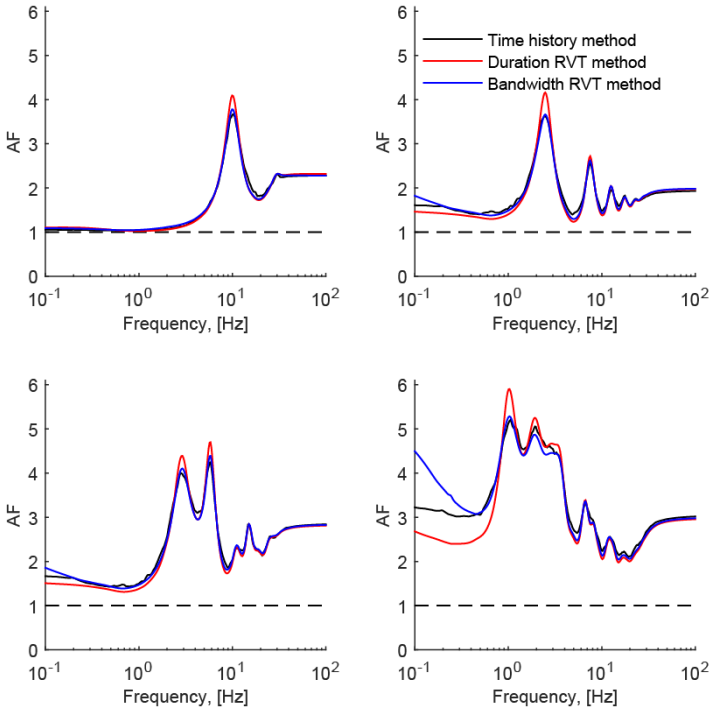

Figure 18. *AF* obtained from each approach for the M5 R30 km scenario. Bandwidth approach uses Case 6 parameters from Table 1. Figures correspond to profiles in Figure 2.

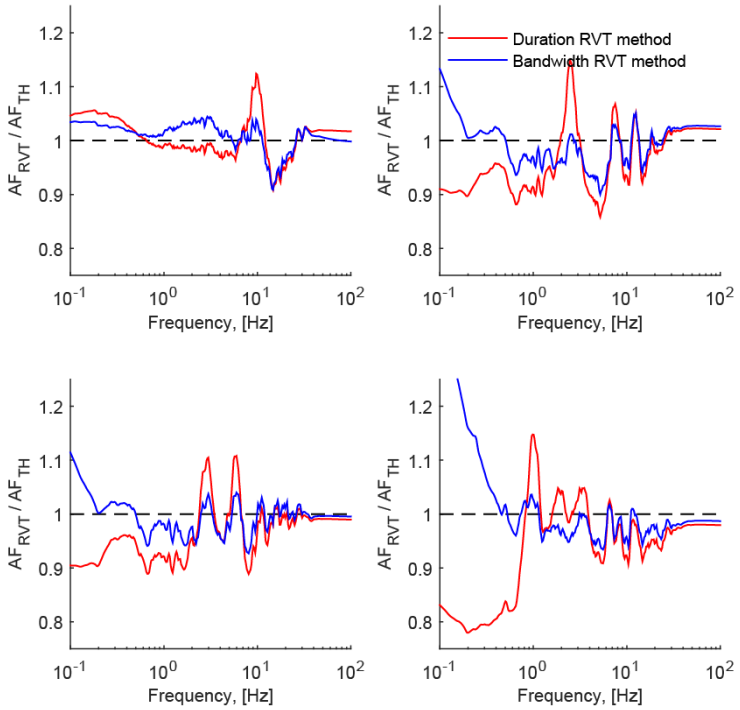

Figure 19. Ratios of *AF* obtained from each RVT approach relative to the time history approach for the M5 R30 km scenario. Bandwidth approach uses Case 6 parameters from Table 1.

4.0 Impact on seismic hazard estimates

The improved agreement between *AF* obtained using RVT and time history site response analysis demonstrated in the previous section is now investigated to determine its impact on probabilistic estimates of seismic hazard. Site response analysis is required for a PSHA when geotechnical conditions at the analyzed site are different from those used to develop the ground motion prediction equations (GMPEs) selected to calculate hazard. It is often the case that site conditions have some degree of uncertainty that must be considered in the analysis. Here, uncertainty in the V_S profile for Site C (Figure 2) is modeled in a manner typical of engineering practice (e.g., EPRI, 2013a). Incorporation of such uncertainty results in a distribution of *AF*, which is assumed to be a lognormal distribution with median $AF_{0.5}$ and logarithmic standard deviation $\sigma_{\ln AF}$. This distribution is convolved with reference "rock" mean hazard curves that have been calculated directly from the GMPEs, and the results are "soil" mean hazard curves specific to the amplification characteristics of the geotechnical model and CPE. This is consistent with Approach 3 of NUREG/CR-6728 (REI, 2001), where the annual probability of exceedance of soil ground motion level *z*, $G_Z(z)$, at a given spectral frequency is computed as:

$$G_Z(z) = \int_0^\infty P\left[AF \geq \frac{z}{x} | x\right] f_X(x)\, dx \qquad 18$$

where $f_X(x)$ is the probability distribution of rock spectral acceleration, which is obtained through differentiation of the rock hazard curve.

In the probabilistic site response analysis performed here, V_S is modeled as a lognormal random variable with median V_S defined by the V_S profile for Site C in Figure 2. The logarithmic standard deviation of V_S is set to 0.15, which is a typical value from EPRI (2013a), and values in each layer are correlated according to the model in Toro (1995). 60 V_S profiles are generated to obtain a stable estimate of the distribution of AF (Figure 20). AF is computed for each of the profile realizations using both the duration and bandwidth (Case 6) RVT approaches and the M7 R30 km scenario (Figure 21), then $AF_{0.5}$ and $\sigma_{\ln AF}$ are computed for each spectral frequency at which hazard will be calculated.

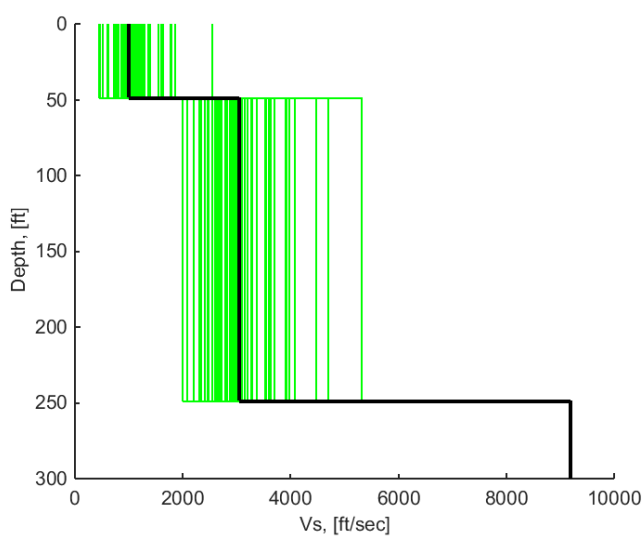

Figure 20. 60 realizations of V_S profiles generated from the M6 R30 km scenario for a probabilistic site response analysis.

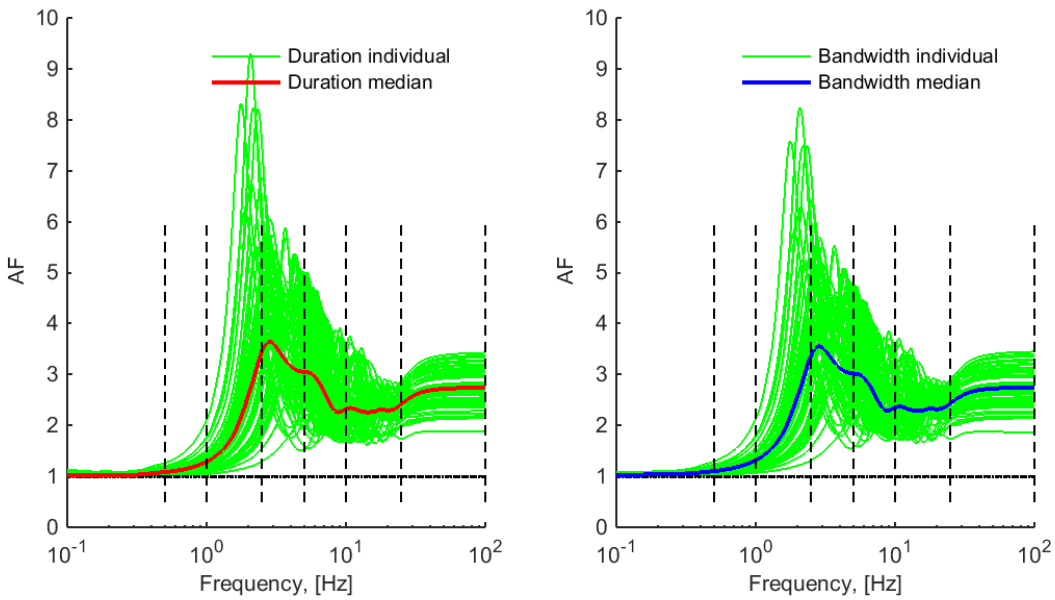

Figure 21. *AF* versus frequency for each of the V_S profile realizations. Spectral frequencies corresponding to the GMPEs used in the PSHA for which $AF_{0.5}$ and $\sigma_{\ln AF}$ are computed are highlighted.

The GMPEs of EPRI (2013b) are used to perform a PSHA at a hypothetical location in the Mid-Atlantic region of the United States. These GMPEs model spectral frequencies of 0.5 Hz, 1.0 Hz, 2.5 Hz, 5.0 Hz, 10 Hz, 25 Hz, and peak ground acceleration (PGA; modeled as 100 Hz) for hard rock (V_S = 9200 ft.sec). Distributions of *AF* are calculated for these seven frequencies, which are highlighted in Figure 21. The values are reported in Table 2 correspond to $AF_{0.5}$ and $\sigma_{\ln AF}$ computed at each of the dashed lines in this figure.

Amplified hazard is calculated using Eqn. 18, rock hazard curves from a PSHA performed for the hypothetical site (which are omitted for brevity), and the distributions of *AF* in Table 2. Note that Eqn. 18 accommodates a dependence of *AF* on *x*, but in this analysis they are treated as independent for simplicity. Uniform hazard response spectra (UHRS) at an annual frequency of exceedence of 10^{-4} are computed from hazard curves for rock, hazard curves for soil obtained using *AF* developed from the duration RVT approach, and hazard curves for soil obtained using *AF* developed from the bandwidth RVT approach (Figure 22). The M7 R30 km scenario is selected for analysis because it is close to a typical mean deaggregated scenario to seismic hazard in the eastern United States for low frequencies and an annual frequency of exceedence of 10^{-4}.

Figure 22 can be viewed in the context of the differences between AF obtained from each RVT approach in Section 3. For the M7 R30 scenario in Figure 15 for Site C, the duration approach predicts greater amplification than the bandwidth approach at the peak amplified frequencies, 2.5 Hz and 5 Hz, by roughly 5%, but it predicts slightly lower amplification at each of the other spectral frequencies analyzed in the PSHA. This translates to lower hazard at 2.5 Hz and 5Hz from the bandwidth approach 22, but greater hazard at the other spectral frequencies. It is important to note that at nearly every frequency in Figure 15 for Site C, the AF from the

bandwidth approach are in better agreement with the time history approach than are AF from the duration approach. This implies that the UHRS computed from the bandwidth approach is also more consistent with what would be calculated from the time history approach.

The ±5% differences in UHRS in Figure 22 are not significant considering the uncertainty in PSHA. For a single spectral frequency at a typical site in the eastern United States, the spread between 16th and 84th fractiles of ground motion amplitude at an annual frequency of exceedence of 10^{-4} is roughly an order of magnitude. These differences are also on the order of the degree of change that may be observed from a fundamentally different site response analysis (e.g., nonlinear time history approach).

Table 2a. *AF* obtained from probabilistic site response analysis using duration RVT approach and the M6 30 km Scenario.

Freq. [Hz]	$AF_{0.5}$	$\sigma_{\ln AF}$
0.5	1.08	0.043
1	1.29	0.134
2.5	3.44	0.403
5	3.05	0.309
10	2.31	0.216
25	2.42	0.108
100	2.74	0.130

Table 2b. *AF* obtained from probabilistic site response analysis using bandwidth RVT approach and the M6 R30 km Scenario.

Freq. [Hz]	$AF_{0.5}$	$\sigma_{\ln AF}$
0.5	1.10	0.044
1	1.32	0.131
2.5	3.36	0.383
5	3.02	0.288
10	2.34	0.203
25	2.44	0.110
100	2.75	0.132

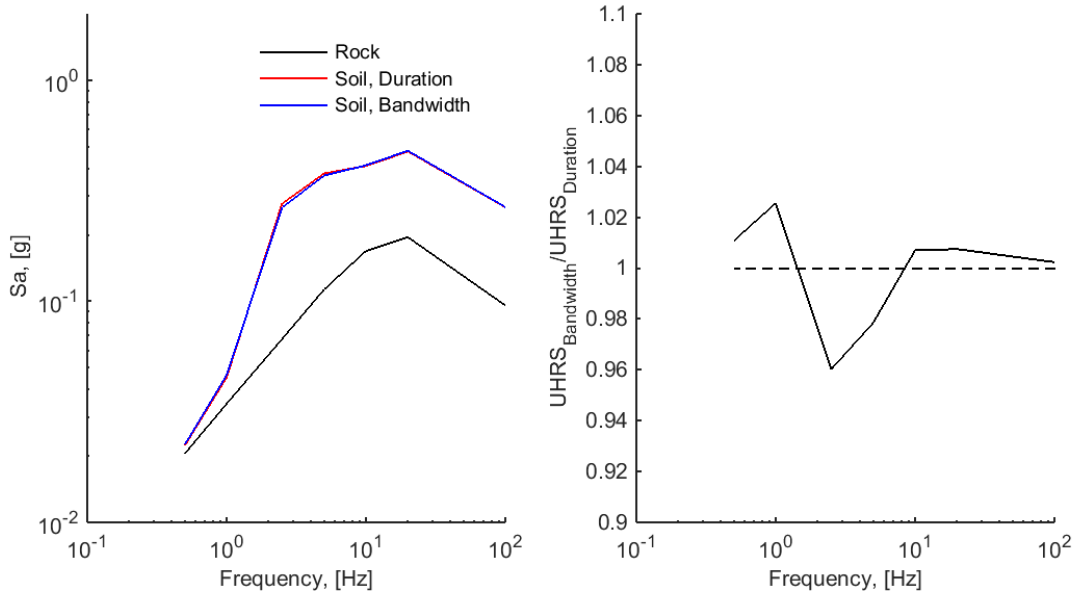

Figure 22. UHRS developed from rock hazard, soil hazard from duration approach, and soil hazard from bandwidth approach.

5.0 Conclusions

The bandwidth approach to RVT site response represents a theoretical alternative to the empirical adjustments made in the duration approach to RVT site response. Several formulations of this alternative approach are considered and tested in order to find a favorable combination of parameters that agree well with *AF* calculated using time histories for a number of different frequency and amplification characteristics via different site conditions and earthquake scenarios. The different formulations each address the nonstationarity of soil-SDOF system responses both at low frequencies and at frequencies strongly amplified by the site.

In a deterministic analysis, the bandwidth approach provides a reduction in peak *AF* relative to the duration approach, resulting in better agreement with *AF* calculated using time histories. Conversely, the bandwidth approach provides an increase in *AF* relative to the duration approach at many other frequencies, although this increase tends to be in better agreement with *AF* calculated using time histories.

When propagated into a probabilistic site response analysis and PSHA, the increases in decreases in amplification from the bandwidth approach relative to the duration approach translate to both increases and decreases in UHRS. The nature of differences in UHRS will depend on the amplification characteristics of the site.

Even though the bandwidth approach addresses the problem of overpredicting amplification at the resonant frequencies of a site, it does not consistently reduce the conservatism of hazard relative to the duration approach. It is important to consider the benchmark for comparison when stating that hazard is over- or under-predicted. In this investigation, *AF* obtained using time history site response analysis are used as the benchmark. The results above suggest that the

duration approach may be underestimating *AF* relative to the time history approach at frequencies not strongly amplified by the site, which may translate to an underestimation of hazard. Future work should include an additional investigation of how hazard obtained via RVT site response analysis compares to other benchmarks, but that is outside the scope of this study.

The results of this investigation suggest that while the bandwidth approach to RVT site response analysis is a theoretically sound alternative to the empirical adjustments of the duration approach, the selection of one or the other in a real-world application will not have a significant impact on the design or retrofit of structures that require the calculation of site-specific hazard.

Limitations of these conclusions include:

- No consideration of existing alternative formulations to the duration approach to RVT site response analysis;
- Limited investigation of different possible geotechnical site characteristics and earthquake scenarios that can influence site response analysis;
- Simplified probabilistic site response analysis that does not vary input rock spectral amplitudes or include a full logic tree per EPRI (2013a).

Each of these limitations is driven mainly by the need to maintain a reasonable scope, and may be easily addressed in the future within the framework developed here.

REFERENCES

Boore, D.M. (2003), "Simulation of ground motion using the stochastic method," *Pure Applied Geophysics*, Vol 160, no.3 635-676.

Boore, D.M. and Joyner, W.B. (1984), "A note on the use of random vibration theory to predict peak amplitudes of transient signals," *Bull. Seism. Soc. Am.*, Vol. 74, pp. 2035-2039.

Boore, D.M. and E.M. Thompson (2012), "Empirical improvements for estimating earthquake response spectra with random vibration theory," *Bull. Seism., Soc., Am.*, Vol. 102, no. 2, 761-772.

Cartwright, D.E. and M.S. Longuet-Higgins (1956), "The statistical distribution of a maximum of a random function," *Proc. Royal Stat Soc*., Vol. 237, pp. 212-232.

Der Kiureghian, A. (1980), "On the response of structures to Stationary Excitiation," Report No. UCB/EERC 79-32, Earthquake Engineering Research Center, University of California, Berkeley, CA.

EPRI, (1988), "Soil response to earthquake ground motion," Electric Power Research Institute, Palo Alto, CA, March.

EPRI, (1993), "Guidelines for determining design basis ground motions," Electric Power Research Institute, Palo Alto, Ca.

EPRI, (2013a), "Seismic Evaluation Guidance Screening, Prioritization and Implementation Details (SPID) for the Resolution of Fukushima Near-Term Task Force Recommendation 2.1: Seismic," Elec. Power Res. Inst. Rept 1025287, Feb.

EPRI, (2013b), *EPRI (2004, 2006) Ground-Motion Model (GMM) Review Project*, Elec. Power Res. Inst, Palo Alto, CA, Rept. 3002000717, June, 2 volumes.

Graizer, V. (2013), "Comment on 'Comparison of time series and random vibration theory site-response methods' by Albert R. Kottke and Ellen M. Rathje," *Bull. Seismol. Soc. Am*. Vol. 104. No. 1, pp 540-546.

Hanks, T.C. and McGuire, R.K. (1981), "The character of high-frequency strong ground motion," *Bull Seis. Soc. Am.*, Vol 71, no. 6, 2071.

Idriss I.M. and J.I. Sun (1992), "SHAKE91: A computer program for conducting equivalent linear seismic response analyses of horizontally layered deposits," *Center for Geotechnical Modeling*, Dept. of Civil and Env. Enggr., University of California, Davis, CA.

Kottke, A. R., and E. Rathje (2013), "Comparison of time series and random vibration theory site-response methods," *Bull. Seism. Soc. Am.* Vol. 103, no. 3, 2111–2127

Kramer S.L. (1996), *Geotechnical Earthquake Engineering*. Prentice Hall, Upper Saddle River, N.J.

Liu L., and S. Pezeshk (1999), “An improvement on the estimation of pseudo-response spectral velocity using RVT method,” *Bull Seis. Soc. Am.*, Vol 89, no. 5, 1384-1389

Rathje, E.M. and Kottke, A.R. (2014), “Reply to ‘Comment on “Comparison of time series and random vibration theory site-response methods’ by V. Graizer, *Bull. Seismol. Soc. Am*. Vol. 104. no. 1, pp. 547-550.

Rathje, E.M. and M.C. Ozbey (2006), “Site-specific validation of random vibration theory-based seismic site response analysis,” *J. Geotech. Geoenv. Eng*., Vol 132, no. 7, 911-922.

Risk Engineering, Inc. (2001), “ Technical basis for revision of regulatory guidance on design ground motions: hazard- and risk-consistent ground motion spectra guidelines”, U.S. Nuclear Regulatory Commission Report, NUREG/CR-6728, October.

Seifried, A.E., and Toro, G.R. (2015). “Improved estimation of site response using random vibration theory”, SSA Annual Meeting, Seismol. Res. Lett. 86, no. 2B, 716–717.

Toro, G.R. (1984), “Probabilistic analysis of combined dynamic responses,” Technical report No. 65, John A. Blume Earthquake Engineering Research Center, Stanford University, Stanford, CA.

Toro, G.R. (1995), “Probabilistic models of site velocity profiles for generic and site-specific ground-motion amplification studies”, Technical Report 779574, Brookhaven National Laboratory, Upton, New York..

Wang, X., and Rathje, E.M. (2016), “Influence of Peak Factors on Site Amplification from Random Vibration Theory Based Site-Response Analyis”, *Bull. Seismol. Soc. Am*. Vol. 106. no. 4, pp. 1733-1746.

Vanmarcke, E.H. (1976), “Structural response to earthquakes,” in *Seismic Risk and Engineering Decisions*, C. Lomnitz and E. Rosenbluth, Editors, Elsevier, Amsterdam.

Final Note: This report is being prepared for submission to the Bulletin of the Seismological Society of America for eventual publication